Vegueta. Anuario de la Facultad de Geografía e Historia
22 (8), 2022
eISSN: 2341-1112
DOI: 10.5281/zenodo.6991856

A THEORETICAL AND EXPERIMENTAL STUDY TO SHOW THE EFFECT OF THERMAL INTERFACE MATERIAL ON THE PERFORMANCE OF A THERMOELECTRIC COOLER

Omar M. Khalaf[1,*], **Thamer Khalif Salem**[1],
[1] Mechanical Engineering Department, Tikrit University, Salah Al-Din, Iraq
omar.m.khalaf43785@st.tu.edu.iq, thamersa1974@tu.edu.iq ; thamer.salem@ozu.edu.tr

Abstract

The advantages of thermoelectric cooling made this type of cooling widely sought by researchers and designers at present. Thus, the study of the thermoelectric cooler has been achieved on the Peltier analysis principle by using different types of thermal interface materials (TIM). Then, the work of the thermoelectric cooler is analyzed under different parameters such as input voltage, cooler loads, and different TIM compared to the thermoelectric cooler without (TIM). The heat dissipation from the heat sinks is analyzed by forced convection. In addition, the theoretical and experimental results have verified a decrease in the temperature of the cold side for the Peltier unit with an increase in voltage with time. As a result, the increase in the amount of absorbed heat leads to an increase in the hot side temperature with incrementing the voltage that accompanied rises of the heat generation on the same side. The experimental results show the minimum and maximum temperatures on the cold surface side of the Peltier element are 272.6 K and 281.4 K for TIM_3 and without TIM respectively, which are got at a voltage of 12 volts. In addition, the system performance using TIM_3 increases by 8.6% compared to the case without TIM at 4 volts. Besides, TIM_3 showed the highest coefficient of performance for the cold side and hot side were 1.04 and 1.97 respectively. Finally, the comparison between the analytical and experimental results achieved a good agreement with a lower variation of less than 14.3%.

Keywords: Thermoelectric cooling, TIM, Peltier element, Heat sink

Nomenclature

A	Area, (m^2)	ΔT	Temperature difference, (K)
Cp	Specific heat, ($KJ \cdot kg^{-1} \cdot K^{-1}$)	***Abbreviations***	
h	Heat transfer coefficient, ($W \cdot m^{-2} \cdot K^{-1}$)	COP	Coefficient of performance, (-)
H	Height, (m)	EX	Experimental, (-)
I	Electric current, (A)	TEC	Thermoelectric cooler, (-)
K	Thermal conductivity ($W \cdot m^{-1} \cdot K^{-1}$)	Th	Theoretical, (-)
ṁ	Mass flow rate ($kg \cdot s^{-1}$)	TIM	Thermal Interface Material, (-)
Q	Heat transfer rate, (W)	***Dimensionless numbers***	
R	Thermal Resistance, ($K \cdot W^{-1}$)	Pr	Prandtl number, (-)
r	Electrical resistance, (Ω)	Re	Reynolds number, (-)
S	Seebeck coefficient, ($V \cdot K^{-1}$)	***Subscripts***	
t	Thickness, (m)	c	Cold side

**Autora de correspondencia / Corresponding author.*

T	Temperature, (K)	h	Hot side
V	The equipped voltage of the device, (v)	i	Inside
ŋ	Efficiency, (%)	o	outer
Greek symbols			

1. Introduction

The increase in global demand for thermoelectric devices is due to the flexibility of their work, where it can work as thermal electric generators. In addition, it is work as coolers that dissipate heat with lower electrical energy consumption. The general trends of modern technology and electronics are to reduce the size of the devices that are used in thermal management cooling systems. Therefore, the scientists began interesting in thermoelectric devices and their manufacturing methods such as the thermoelectric refrigerator for utilizing in the local and global market. In 2016, Thakkar Mohit[1] studied traditional cooling and the non-proliferation of Peltier cooling, which works on thermoelectric parts. The results showed reducing irreversible processes that lead to increased efficiency and reduced losses. In addition, the thermoelectric cooling systems were analyzed with design description by Raghied M. Atta[2], 2018. A summary of thermoelectric cooling technologies with governing equations was presented and defining all the design parameters of thermoelectric cooling devices to increase the system performance. The solar thermoelectric chillers were proposed using in low-energy environments. In addition, the pilot study for performance evaluation and thermodynamic modeling of a thermoelectric cooler type TEC-12704 with two heat sinks was investigated by Marzieh Siahmargoi [3] et al., 2019. The comparison results between the theoretical and the experimental results gave a good agreement with low variation. The thermal resistance results of both TEC sides had an inverse effect on the thermoelectric cooler performance. In addition, Uri Lachish [4] 2020 studied the thermoelectric effects of Peltier, Seebeck, and Thompson on the thermoelectric cooler performance. A simple model was created to derive the equations for the electrothermal effect. Then, the results showed that the Thomson effect occurs in the steady state of heat flow instead of the state of equilibrium. Besides, the electromotive force resulting from the Seebeck effect changes linearly with temperatures. Frankia Meng et al., 2008 [5] studied analytically for improving the performance of a two-stage thermoelectric cooling system. The TEC model was built and the analytical study was achieved by deriving the governing equations. In addition, the thermoelectric elements were achieved for optimizing the maximum enhancement in cooling load and COP. The results proved that the increase in the number of thermocouples leads to an increase in the cooling load and system performance. In 2012, Mayank Awasthi et al. [6] studied the design and development of the thermoelectric refrigerator. The study aimed to develop a thermoelectric refrigerator with a cooling capacity of 5 liters. The theoretical results demonstrated the temperature inside the refrigerator remains up to 52 minutes after the power is cut off from the refrigerator. A review on the improvement of the thermal heat sinks design had been demonstrated by Hamdi E. Ahmed et al, 2018 [7]. The thermal design of heat sinks was enhanced by considering different parameters such as examining the heat transfer rate, fin shapes and directions, inlet and outlets of heat sinks, fixed and rotating of the heat sinks, and substrate materials type of the heat sink thermal. Finally, The main objective of this study was to summarize the research efforts that have been made to develop the thermal performance of heat sinks, limitations, and unresolved proposed solutions. The optimization of the operating conditions of the thermoelectric refrigerator and analyzed its performance under optimal conditions were studied by Ahmet

Caglar et al., 2018 [8]. The boundary conditions of the theoretical calculations had been analyzed at the Peltier element voltage is 12V, the indoor and outdoor fans are 3V and 9V respectively, and the ambient temperature is 293 K. The results showed of the temperature inside the refrigerator decreased from 293 K to 254.8 K, and the performance factor was 0.011. The theoretical utilization of exhaust gases for the cooling process was investigated by Simon Chinguwa et al. [9]. A thermoelectric generator system is used to recover the waste heat from the exhaust gases, which is designed to operate as a thermoelectric refrigerator.

In this study, a thermoelectric type (TEC-12706) is analyzed by using two heat sinks that can be dissipated the heat by forced convection on the cold and hot sides of TEC; as well as to prevent the refrigeration unit from being damaged by exceeded heat.

2. Mathematical Analysis

The thermoelectric cooler consists of two semiconductor elements that are combined by conductive strips to manufacture a thermoelectric cooler (see Figure 1). The dual of TEC can be classified into a positive (p) and negative (N), when the electric current is connected to the TEC led to be one side is hot and the other side is cold depending on the direction of the current. This phenomenon of the hot and cold sides is occurred in TEC due to the transfer of electrons and holes from the positive part (P) to the negative part (N) at the electric current passes through the cooler [10]

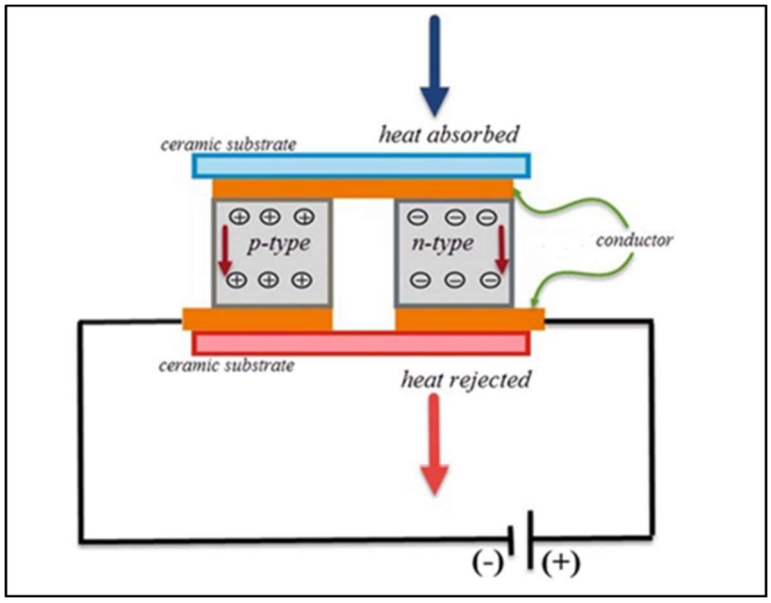

Figure (1): show the components of the thermoelectric cooler [3]

The heat absorbed on the cold side and generated on the hot side that can be calculated by following the equations [11], [12], [13], [14], ,[15] and[16] :

$$Q_c = \mathrm{S}\, T_c\, I - 0.5\, I^2 r - \mathrm{K}\, \Delta \mathrm{T} \qquad (1)$$

$$Q_h = \mathrm{S}\, T_h\, I - 0.5\, I^2 r - \mathrm{K}\, \Delta\mathrm{T} \quad (2)$$

In addition, the temperature of the hot side and the cold side can be computed from the following equations [3], [17], [18]:

$$T_c = \frac{T_i + 0.5\, I^2\, r\, R_C + \mathrm{K}\, \Delta\mathrm{T}\, R_C}{\mathrm{S}\, \mathrm{I}\, {R_C}^{-1}} \quad (3)$$

$$T_h = \frac{T_o + 0.5\, I^2\, r\, R_h + \mathrm{K}\, \Delta\mathrm{T}\, R_h}{1 - \mathrm{S}\, \mathrm{I}\, R_h} \quad (4)$$

$$\Delta\mathrm{T} = T_h - T_c \quad (5)$$

The supplied current is analyzed theoretically based on the third-order equation as follows [3]:

$$(\mathrm{S}^2\, r\, R_h R_C) I^3 - (\mathrm{S}^2\, V\, R_h R_C - \mathrm{S}\, \mathrm{r}\, (R_h - R_C) - 0.5\, r\, \mathrm{S}(R_h + R_C)) I^2 - (\mathrm{S}^2 R_C (T_o + T_i) - r\, \mathrm{K}(R_h + R_C) + r + \mathrm{S}\, \mathrm{V}(R_h - R_C)) I - (\mathrm{K}(R_h + R_C) - 1) V = 0 \quad (6)$$

Then, the supplied voltage and input power are determined by [3]:

$$V = \mathrm{S}\, \Delta T + r\, I \quad (7)$$

$$Q_{in} = V \times I \quad (8)$$

As a result, the performance coefficient of the thermoelectric unit is estimated from [14]

$$\mathrm{C}OP = \frac{Q_c}{Q_{in}} \quad (9)$$

$$COP_h = \frac{Q_h}{Q_{in}} \quad (10)$$

It is noteworthy that the Seebeck coefficient can be evaluated by [19]:

$$\mathrm{S} = \frac{\mathrm{S}_{\mathrm{T}_h} - \mathrm{S}_{\mathrm{T}_C}}{\Delta\mathrm{T}} \quad (11)$$

Also, the electrical resistance and conductivity are calculated as follows [19]:

$$\mathrm{r} = \frac{\mathrm{r}_{\mathrm{T}_h} - \mathrm{r}_{\mathrm{T}_C}}{\Delta\mathrm{T}} \quad (12)$$

$$\mathrm{K} = \frac{\mathrm{K}_{\mathrm{T}_h} - \mathrm{K}_{\mathrm{T}_C}}{\Delta\mathrm{T}} \quad (13)$$

The heat generated on the hot side increases with the operation time of the thermoelectric cooler. An increment in the hot side heat leads to get a melting in the thermocouple and thus damage to the coolant. Therefore, a heat sink and an air fan were combined (see Figure 2) on the hot side for dissipating the exceeded heat; and on the cold side to distribute the low temperature inside the cooling region.

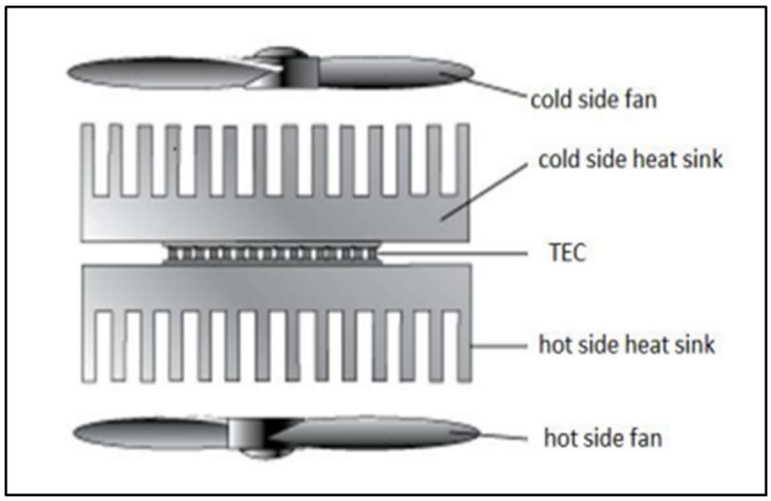

Figure (2): shows the method of connecting the thermoelectric device [10]

To determine the amount of heat that is dissipated from the heat sinks as follows [20], [21]:

$$Q_{total} = \frac{T_{TEC} - T_{out}}{R_{total}} \quad (14)$$

The overall thermal resistance R_{total} can be calculated by analyzing the TEC (see Figure 3) [20]

$$R_{total} = R_{TEC} + R_{base} + R_{TIM} + \left\{\frac{1}{R_{fin}} + \frac{1}{R_{un-finned}}\right\} + R_{flow} \quad (15)$$

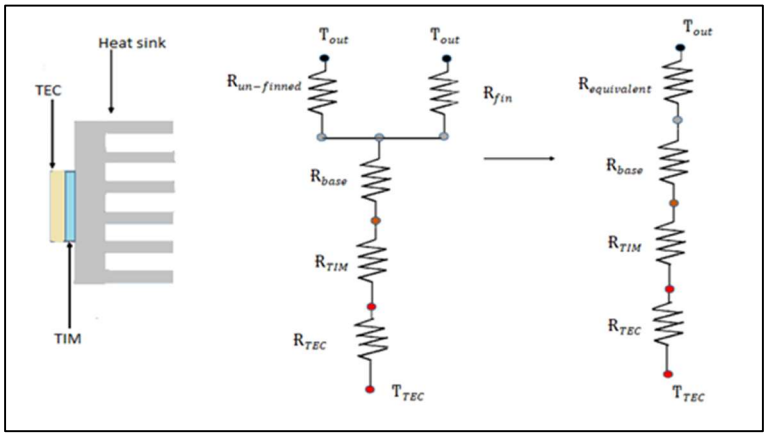

Figure(3): Schematic diagram of the thermal resistance [20]

Where the thermal resistance for each component of TEC can be calculated separately as follows [20], [22], [23], and [24]:

First, the thermal resistance of the thermoelectric cooler is determined as follows:

$$R_{TEC} = \frac{t_{TEC}}{A_{TEC}\, K_{TEC}} \quad (16)$$

The thermal resistance of the thermal interface material is calculated by:

$$R_{TIM} = \frac{t_{TIM}}{A_{TIM}\, K_{TIM}} \quad (17)$$

The thermal resistance of the heat sink base is given by[20],[17] :

$$R_{base} = \frac{t_{base}}{A_{base}\, K_{base}} \quad (18)$$

Thermal resistances of fin and un-finned can be obtained [20]:

$$R_{fin} = \frac{1}{h_{fin}\eta_{fin}A_{fin}} \quad (19)$$

$$R_{un-finned} = \frac{1}{h_{un-finned}A_{un-finned}} \quad (20)$$

Finally, the thermal resistance of the airflow through the heat sink can be calculated from the equation below:

$$R_{flow} = \frac{1}{\dot{m}_{air}\, C_{p_{air}}} \quad (21)$$

The heat transfer coefficient of fin and un-finned can be calculated as follows:

$$h_{fin} = \frac{K_{air}}{A_{s-fin}} \times 0.664\, Re_{air}{}^{1/2} \cdot Pr_{air}{}^{1/3} \quad (22)$$

$$h_{un-finned} = \frac{K_{air}}{A_{s-un-fin}} \times 0.664\, Re_{air}{}^{1/2} \cdot Pr_{air}{}^{1/3} \quad (23)$$

The fin efficiency can also be estimated by [25]:

$$\eta_{fin} = \frac{\tanh ß}{ß} \quad (24)$$

Where $ß = H_{fin} \times \{\frac{2h_{fin}}{K_{AL} * t_{fin}}\}^{0.5}$ (25)

3. Arithmetic program

The thermoelectric cooler is analyzed theoretically to predict the thermoelectric cooler work and estimate the main parameters that affect the TEC. The theoretical study is investigated by using the EES program to obtain the theoretical results such as temperature, amount of heat, and the performance factor of the TEC. The analysis is based on different parameters such as the input voltage, ambient temperature, thermal Interface material TIM, cooling load, and air velocity. The analytical calculation is illustrated in the algorithm diagram in Figure (4).

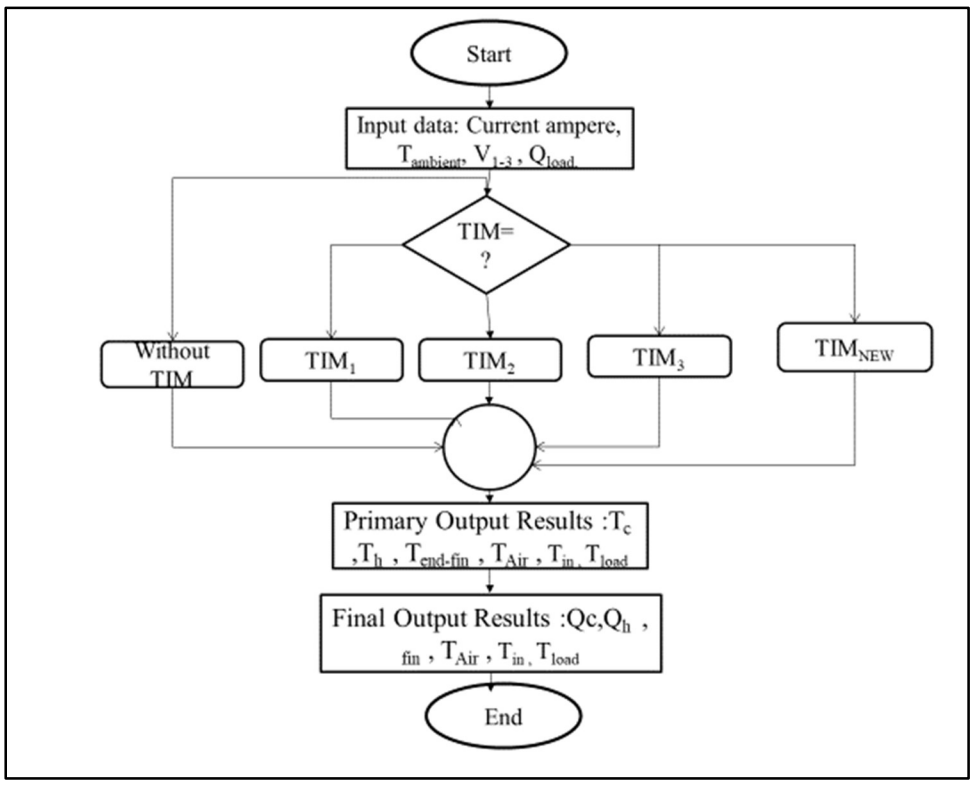

Figure (4): the schematic algorithm of the Arithmetic program

4. The experimental Part

The laboratory experiment basics depend on several parameters to obtain the required results, which is the refrigerator work with the change in the thermal interfacial material type (TIM) compared to the test case without TIM. In addition, the experimental tests were achieved in five cases, one without the use of TIM and three of them depending on different types of TIM. Besides, the fifth case (TIM_{new}) is prepared by mixing different ratios from the three thermal materials 1:2:7 for each of TIM_1, TIM_2, and TIM_3, respectively, and their properties are shown in Table (4). The second parameter was the voltage that is supplied to the TEC from 4 volts to 12 volts, which in turn leads to a change in the supplied current to the TEC, with measuring the ambient and refrigerator temperature before starting the tests. The temperatures were measured by using thermocouples type (K) (see Table 1) on different locations of the system rig at each surface side of the thermoelectric cooler, the heat sinks fins tips, inside the refrigerator, and the temperature change of the load thermal. As a result, these temperatures had been used to calculate the heat transfer rate in the cold side Q_c and the hot side Q_h, and the performance coefficient COP. For more explanation, the experimental device is a refrigerator operating on the Peltier principle of electrothermal cooling with two heat sinks on both sides that as shown in Figure (5). The test rig is based on forced convection to transfer the extra heat by using fans on both sides of TEC. In addition, figure (6) demonstrates the experimental device of the thermoelectric refrigerator TER and the measuring devices that are used to conduct the experimental tests.

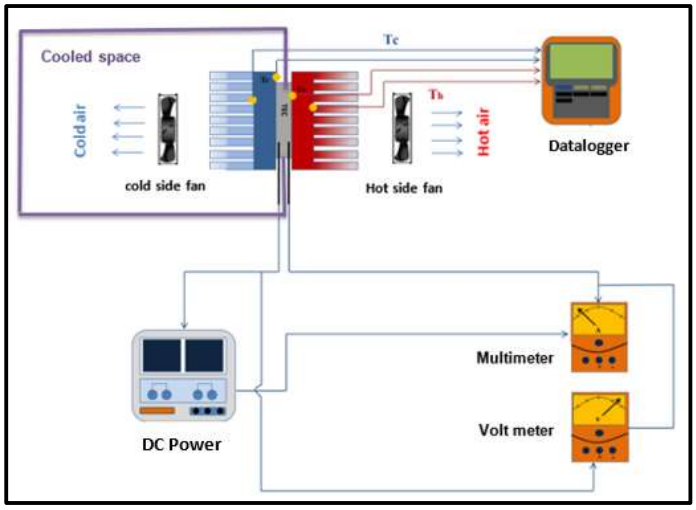

Figure (5) shows the schematic diagram of the practical device with the measuring devices

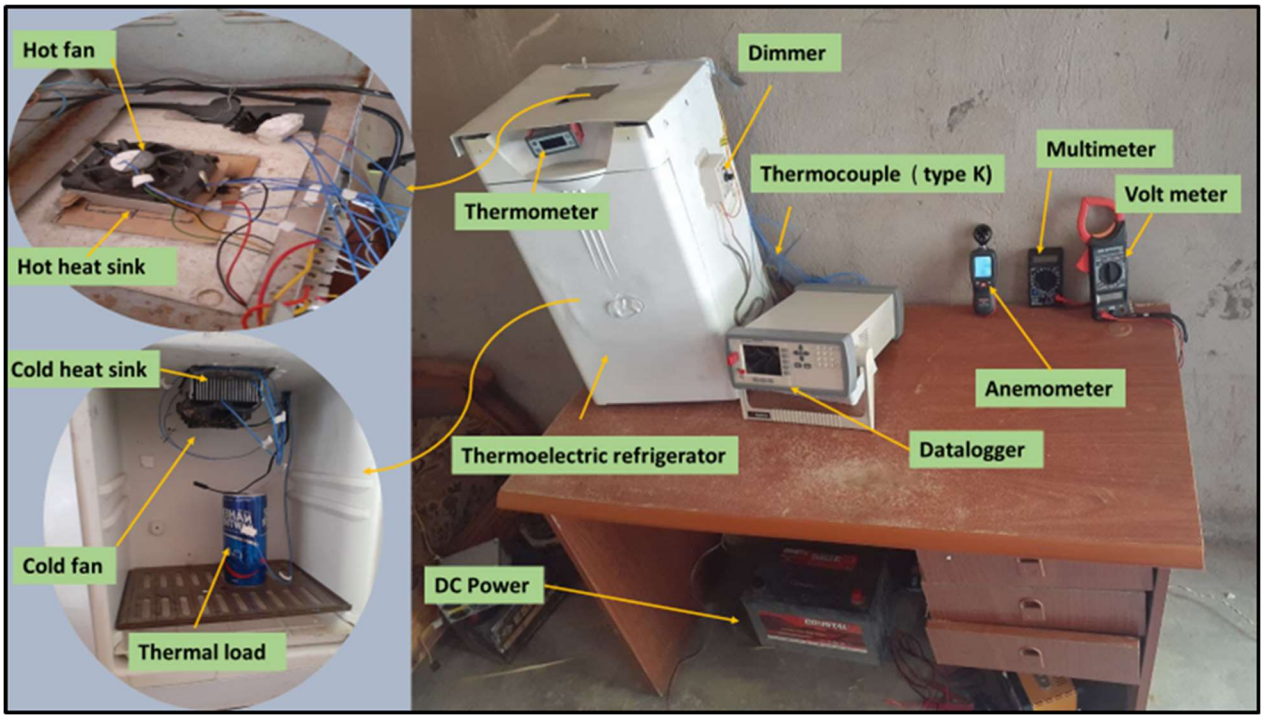

Figure (6): shows the practical test device with measuring devices

Table 1 shows the details of the measuring devices used in practical calculations

Parameter	Value
Thermoelectric modules	
Model	TEC1-12706
Dimension	40mm×40mm×3.8mm
Data logger	
Model	Applent AT4516
Number of channels	16 channel
Temperature sensor	
Type	K
fan	
Model	F08G-12B2S1
P/N	A80856-004
DC Voltage	12V
DC Current	0.28A

5. Results and Discussion

The computational aspect of this study depends on the change of different parameters such as the thermal Interface material, voltage, and heat load. The main variables are accompanied by other changes that are used to determine the work and performance of the thermoelectric cooler. Then, the main characteristics of the study are shown in Table (2) and the output results are based on these characteristics. Consequently, the summary of the results illustrated the temperature on the cold surface of the Peltier element (T_c) decreases with incrementing the voltage, while the temperature on the hot side (T_h) rises with increasing voltage. In addition, the dispersion rate of heat transfer from the heat sink is directly proportional to the surface temperature of the Peltier element. And Table (3) shows the properties of the heat sink used in this study.

Table (2): Shows the main characteristics of initial boundary conditions

T_i (K)	T_o (K)	S ($v \cdot K^{-1}$)	r ($K \cdot W^{-1}$)	K ($W \cdot m^{-1} \cdot K^{-1}$)
298	298	0.05325	2.4	0.5266

Table (3): Demonstrated the specification of the heat sink

Material	Type	Dimension (mm)	Fins Number (-)
Aluminum	Rectangular	84×68×32	20

The calculations were achieved for five cases, the first case was performed in the absence of the thermal interfacial material TIM, while the remaining three cases depend on three materials with different properties such as thermal conductivity and resistance (see Table 4). Hence, the fifth case of the new thermal interface material TIM_{new} is prepared by mixing the other TIM_{1-3} at variables weight percentages of 10%, 20%, and 70% for TIM_1, TIM_2, and TIM_3 respectively (see Equ. 26).

$$TIM_{new} = 10\%TIM_1 + 20\%TIM_2 + 70\%TIM_3 \quad (26)$$

Table (4): Showed the thermal conductivity and resistance of all thermal Interface materials

Thermal interface material	TIM_1	TIM_2	TIM_3	TIM_{New}
Type	HC-151	HF-190	HY610	---
Conductivity ($^{w}/_{m.k}$)	1.2	1.9	3.05	2.63
thermal resistance K/W	0.225	0.225	0.073	0.1186

The surface temperatures on both sides of the thermoelectric cooler using various TIM are also illustrated in Table (5) at changing the voltages from 4 volts to 12 volts. The temperature results showed that the lowest T_c and highest T_h are obtained in the fifth case (TIM_{new}) at 12 volts compared to the other ones.

Table (5): Demonstrated the surface temperatures T_c and T_h on each side of the thermoelectric cooler

NO.	Voltage (v)	Theoretical		Experimental		T_c Error percentage (%)	T_h Error percentage (%)
		T_c (K)	T_h (K)	T_c (K)	T_h (K)		
1	4	277.2	311	280	308	1.01	0.97
2	6	275.6	314	278.7	312	1.12	0.6
3	8	273.8	319.8	277	317	1.16	0.88
4	10	271	324	275	321	1.47	0.93
5	12	269.2	331.5	273.7	327.3	1.7	1.28

Figure (7) shows the relationship between the cold surface temperatures T_c of the thermoelectric cooler with the electric potential difference V. The results illustrate the decrease in T_c with an increase in the voltage due to an increment in the heat absorbed on the cold side of the thermoelectric cooler. The lowest cold temperature achieved at 12 Volt for theoretical and experimental analysis is 269.2 K and 273.8 K respectively. According to the Peltier principle, when electric power passes through the thermoelectric cooler lead to generate a temperature difference on both sides of the thermoelectric cooler, and the temperature difference increases with the increase of that power. The highest difference between the practical and theoretical results of T_c is 1.78% at 12 Volt. In addition, the temperature results of the current thermoelectric cooler TEC-12706 are validated by comparing it with a TEC-12704 [3], which gave the same behavior at the ranging of input voltage from 4 Volts to 14 Volts. Correspondingly, TIM_3 gave the highest rising in Tc by 1.2%, 1.3%, and1.6% compared to the TIM_2, TIM_1, and without TIM respectively because the TIM_3 type has the largest value of thermal conductivity (K= 3.05 w/m·K) than the other TIM types.

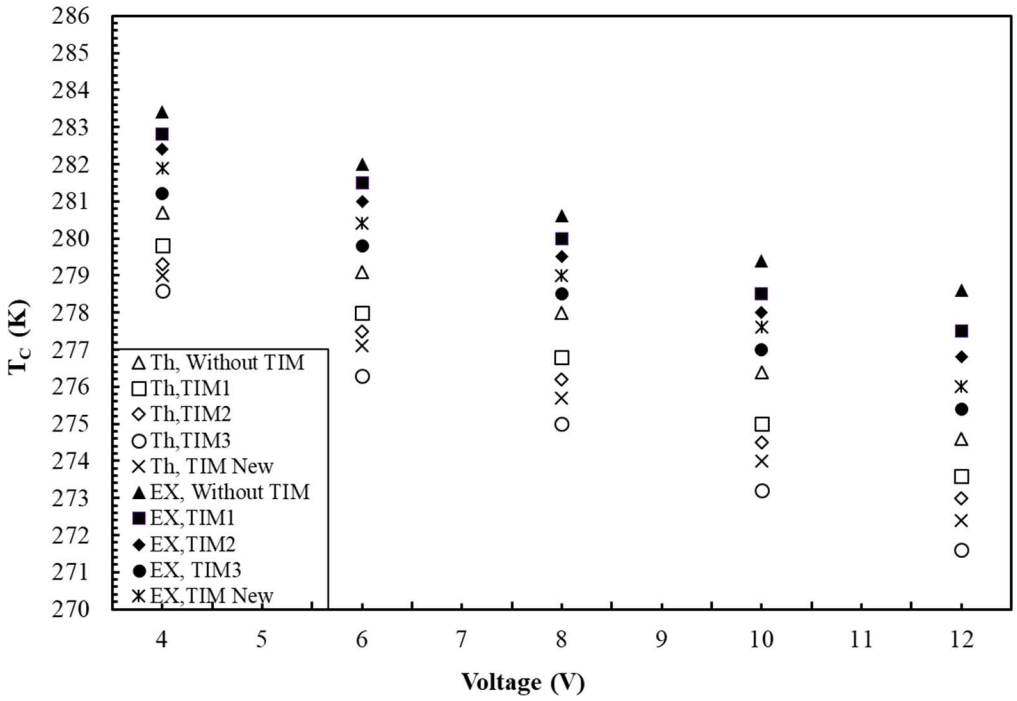

Figure (7): Shows the temperature change on the surface of the cold side scattering with the change of voltage at the difference of the TIM

The effect of the electric potential difference V on the hot surface temperature T_h of the thermoelectric cooler is presented in Figure (8) with different TIM. The behavior of the hot surface temperatures is in the opposite trend compared to the cold surface temperature (see Figure 7). Then, the hot surface temperature increments with the increase in the voltage because of rising in the current and the electromotive force entering the thermoelectric cooler. For more explanation, the hot surface temperatures of the thermoelectric cooler are directly proportional to the electromotive force supplied to the thermoelectric cooler. The highest hot surface temperature is obtained at 12V, where it theoretically amounted to 331.5 K and experimentally is 327.3 K. In addition, the results show that using TIM_3 gives the largest incrementing of T_h are 0.5%, 0.8%, and 1.3% compared to the TIM_2, TIM_1, and Without TIM, respectively.

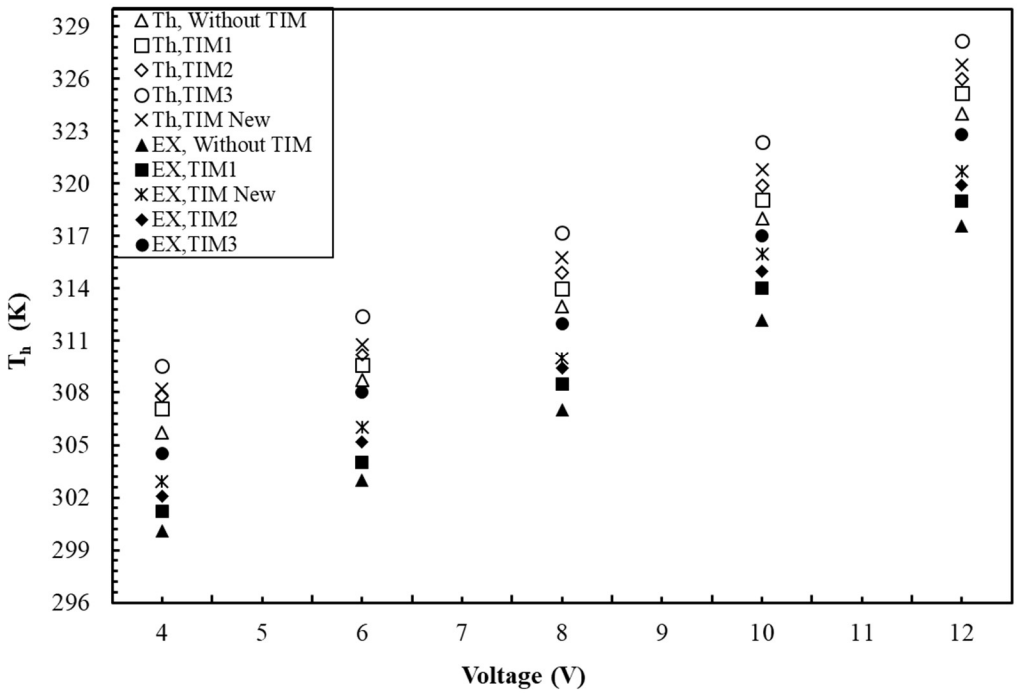

Figure (8): Shows the change of hot temperatures on the surface of the heated side scattering with the change of voltage at the difference of the TIM

The impact of the voltage V on the amount of heat energy absorbed from the cold side Q_c of the thermoelectric cooler is shown in Figure (9). The results showed an increase in the heat transfer rate with rises in voltage V due to an increment in the input power to the TEC. In addition, the experimental results illustrated increasing of Q_c using TIM_3, TIM_{new}, TIM_2, and TIM_1 by 16.7%, 13.3%, 10.8%, and 7.5%, respectively, compared without interfacial material. This is because TIM_3 has the highest thermal conductivity and lowest thermal resistance (see Table 4) than the other types of TIM, which leads to reduce the Obstacles and thermal losses in the contact area between the heat sink and the TEC. As a result, the maximum variation of Q_c is achieved between the practical and theoretical results 11.14% for TIM_3 at 4 Volt. Finally, The current results of Q_c are compared for the TEC-12706 with the TEC-12704 [3] offering the same behavior at the voltage supplied from 4 volts to 12 volts.

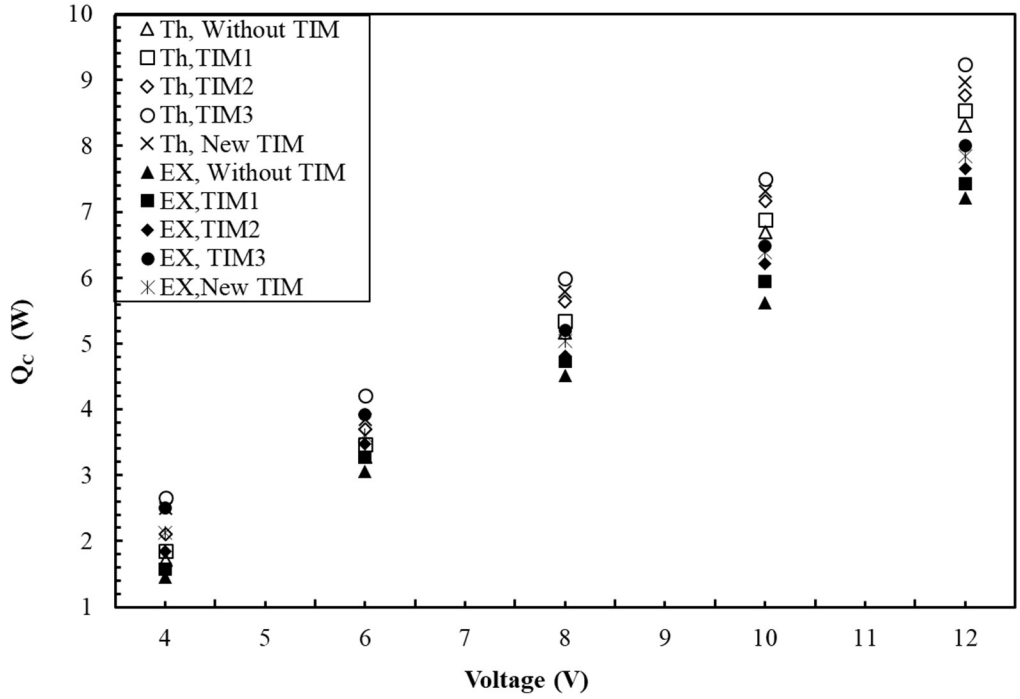

Figure (9): It shows the change in the amount of energy absorbed on the cold side scattered with voltage when the differs TIM.

The amount of heat emitted Q_h from the hot side of the TEC versus the input voltage is represented in Figure (10). The results showed an increase in the input power and the amount of the dissipation heat Q_h with the incrementing in input voltage. Then, the practical results demonstrated rising in dissipation heat Q_h from the hot side of TEC using TIM_3, TIM_{new}, TIM_2, and TIM_1 by 16%, 12.14%, 7.5%, and 5.69%, respectively, compared to the experimental test without TIM. Consequently, the thermal interface material TIM_3 presented the slightest difference between the theoretical and practical results of Q_h by 14% at 4V.

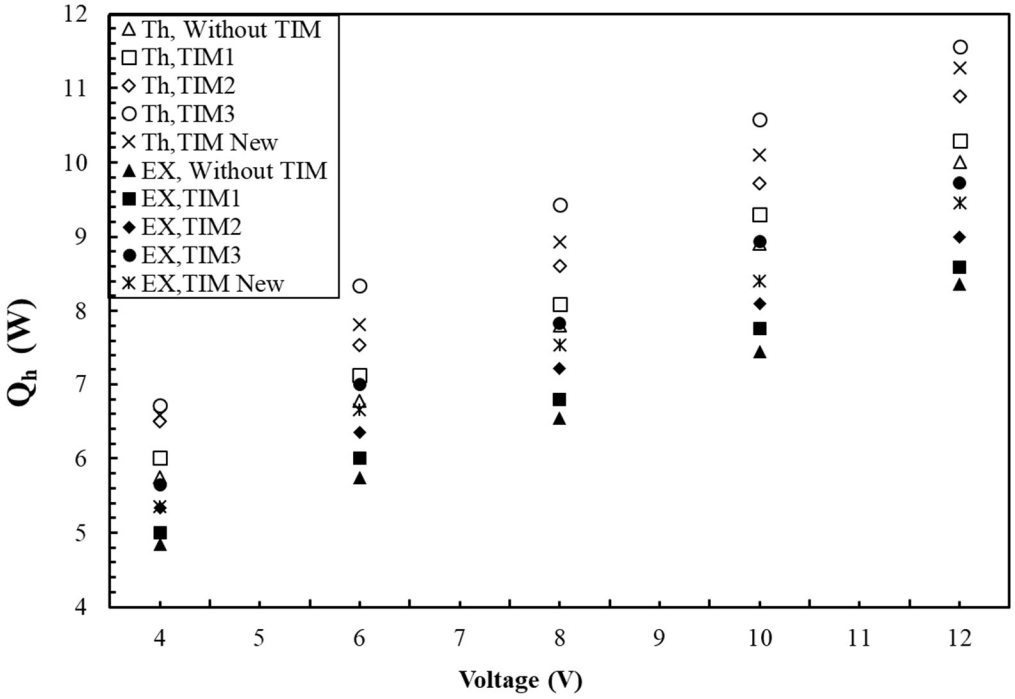

Figure (10): It shows the change in the amount of heat emitted from the heated side with the change in the voltage when using different TIM.

In addition, figure (11) shows the effect of voltage V on the performance coefficient of the cold side COP_c for the TEC with different types of TIM. The results illustrated decreasing the COP_c as rising in voltage from 4 volt to 12 volt due to an increase in the heat losses from the system with the incrementing of input power. As a result, the relationship of COP_c is inversely proportional to the cooling capacity in the refrigerator and directly proportional to the amount of absorption heat of the TEC cold side. Besides, TIM_3 gave the highest performance of TEC for the cold side because it has larger thermal conductivity than the other types of TIM that can be absorbed the biggest amount of heat. In addition, the highest performance for the cold side of the TEC that is achieved theoretically and experimentally is 1.12 and 1.04 respectively by using TIM3 at 4 volts. The current results of Q_h are validated by comparing with the thermoelectric cooler type TEC-12704 [3], which offered a similar trend at the same change of voltage from 4 volts to 12 volts.

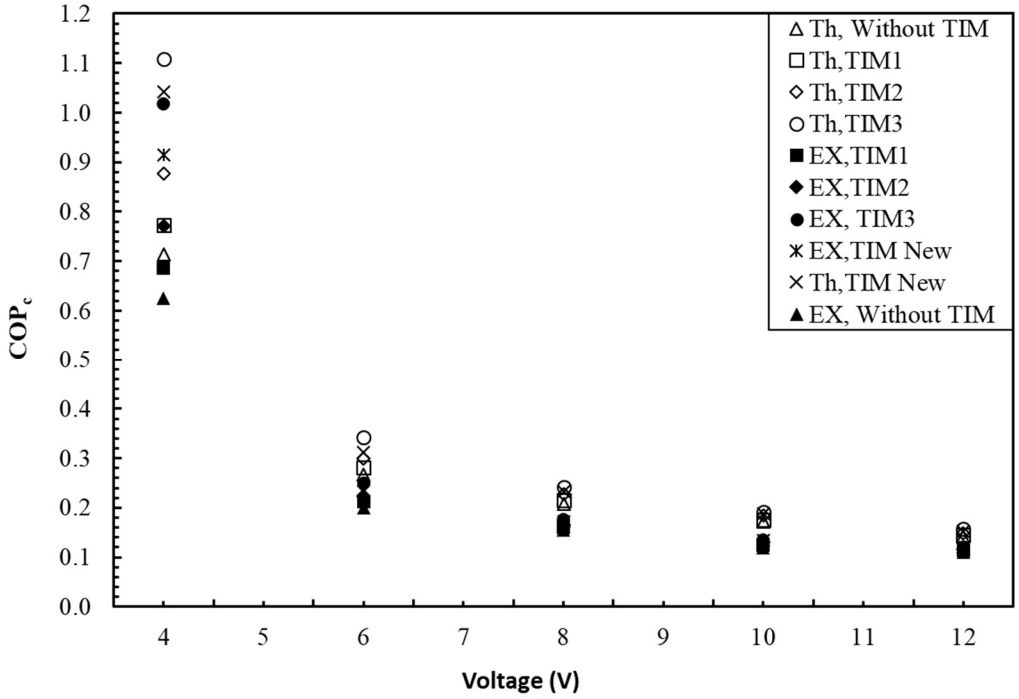

Figure (11): It shows the COP of the cold side of the TEC with the change in the voltage when using different TIM.

Finally, figure (12) show the variation of performance coefficient in the hot side of the thermoelectric cooler with voltage V using different types of TIM. The performance of the hot side offered the same behavior of COP_c (see figure 11), which is decreasing with increasing the voltage for all cases due to rising heat losses and input power. In addition, the results demonstrated that the hot side performance coefficient of the TEC is higher than the cold side performance because the amount of heat emitted from the hot side is larger than the amount of heat absorbed on the cold side. Then, the analytical and experimental results presented the largest COP_h are 2.1 and 1.97 respectively when using TIM_3 and 4 volts. This is because the TIM_3 can transfer the biggest amount of heat emitted from the TEC-hot side to the heat sink due to it has high thermal conductivity compared to the other ones. Finally, the experimental results of COP_h are lower than the theoretical COP_h due to increasing the heat losses from the TEC-hot side, which are neglected in the theoretical calculations.

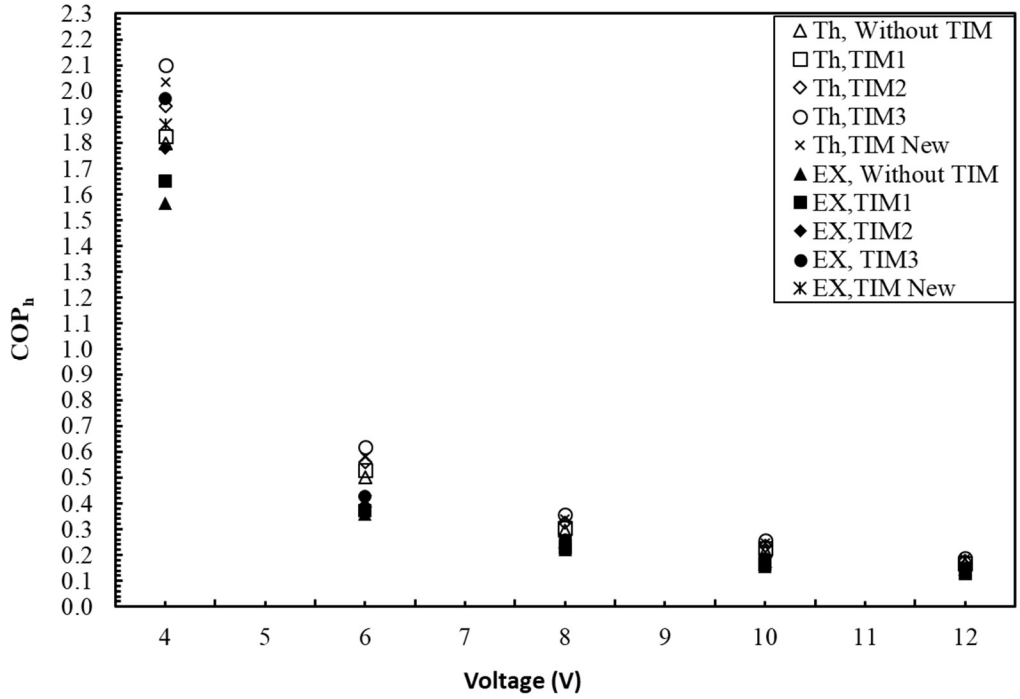

Figure (12): Shows the change in the COP of the hot side of the TEC with the change in voltage and the TIM.

6. Conclusion

This study was conducted theoretically and experimentally to determine the effects of changing both voltage and TIM on the performance of TEC using two heat sinks. The main achievement of this study can be summed up as follows:

1. Using TIM led to an increment in the thermal conductivity and lessens the thermal resistance between the heat sink and TEC.
2. Improving the thermal conductivity of TIM leads to increasing each parameter as T_h, Q_c, Q_h, COP_c, and COP_h.
3. Expanding the voltage leads to an increment in T_h, Q_c, and Q_h.
4. An increase in voltage is accompanied by a reduction of T_c, COP_c, and COP_h.

Acknowledgments

The manuscript organizers would like to thank the help of Tikrit University/college of engineering / mechanical engineering department for completing this manuscript.

References

[1] M. Thakkar, T. M. Pravinchandra, and J. Patel, "A report on 'Peltier (thermoelectric) cooling module' Peltier Cooling Module," 2016, doi: 10.13140/RG.2.1.2923.8805.

[2] R. M. Atta, "Thermoelectric Cooling," in *Bringing Thermoelectricity into Reality*, InTech, 2018. doi: 10.5772/intechopen.75791.

[3] M. Siahmargoi, N. Rahbar, H. Kargarsharifabad, S. E. Sadati, and A. Asadi, "An Experimental Study on the Performance Evaluation and Thermodynamic Modeling of a Thermoelectric Cooler Combined with Two Heatsinks," *Scientific Reports*, vol. 9, no. 1, Dec. 2019, doi: 10.1038/s41598-019-56672-9.

[4] Uri Lachish, "Thermoelectric Effect Peltier Seebeck and Thomson," 2020, doi: 10.13140/RG.2.2.25436.13444.

[5] F. Meng, L. Chen, and F. Sun, "Performance optimization for two-stage thermoelectric refrigerator system driven by two-stage thermoelectric generator," *Cryogenics (Guildf)*, vol. 49, no. 2, pp. 57–65, Feb. 2009, doi: 10.1016/j.cryogenics.2008.11.005.

[6] M. Awasthi and K. v Mali, "DESIGN AND DEVELOPMENT OF THERMOELECTRIC REFRIGERATOR," 2012. [Online]. Available: http://www.ijmerr.com/currentissue.php

[7] H. E. Ahmed, B. H. Salman, A. S. Kherbeet, and M. I. Ahmed, "Optimization of thermal design of heat sinks: A review," *International Journal of Heat and Mass Transfer*, vol. 118. Elsevier Ltd, pp. 129–153, Mar. 01, 2018. doi: 10.1016/j.ijheatmasstransfer.2017.10.099.

[8] A. Çağlar, "Optimization of operational conditions for a thermoelectric refrigerator and its performance analysis at optimum conditions," *International Journal of Refrigeration*, vol. 96, pp. 70–77, Dec. 2018, doi: 10.1016/j.ijrefrig.2018.09.014.

[9] S. Chinguwa, C. Musora, and T. Mushiri, "The design of portable automobile refrigerator powered by exhaust heat using thermoelectric," in *Procedia Manufacturing*, 2018, vol. 21, pp. 741–748. doi: 10.1016/j.promfg.2018.02.179.

[10] J. Patel, M. Patel, J. Patel, and H. Modi, "Improvement In The COP Of Thermoelectric Cooler," *INTERNATIONAL JOURNAL OF SCIENTIFIC & TECHNOLOGY RESEARCH*, vol. 5, p. 5, 2016, [Online]. Available: www.ijstr.org

[11] Y. Zhou and J. Yu, "Design optimization of thermoelectric cooling systems for applications in electronic devices," in *International Journal of Refrigeration*, Jun. 2012, vol. 35, no. 4, pp. 1139–1144. doi: 10.1016/j.ijrefrig.2011.12.003.

[12] H. Lee, *Thermal design : heat sinks, thermoelectrics, heat pipes, compact heat exchangers, and solar cells*. Wiley, 2010.

[13] M. Yamanashi, "A new approach to optimum design in thermoelectric cooling systems," *Journal of Applied Physics*, vol. 80, no. 9, pp. 5494–5502, Nov. 1996, doi: 10.1063/1.362740.

[14] D. Zhao and G. Tan, "A review of thermoelectric cooling: Materials, modeling and applications," *Applied Thermal Engineering*, vol. 66, no. 1–2. pp. 15–24, May 2014. doi: 10.1016/j.applthermaleng.2014.01.074.

[15] J. Mardini-Bovea, G. Torres-Díaz, M. Sabau, E. De-La-hoz-Franco, J. Niño-Moreno, and P. J. Pacheco-Torres, "A review to refrigeration with thermoelectric energy based on the peltier effect," *DYNA (Colombia)*, vol. 86, no. 208, pp. 9–18, 2019, doi: 10.15446/DYNA.V86N208.72589.

[16] J. Mardini-Bovea, G. Torres-Díaz, M. Sabau, E. De-La-hoz-Franco, J. Niño-Moreno, and P. J. Pacheco-Torres, "A review to refrigeration with thermoelectric energy based on the peltier effect," *DYNA (Colombia)*, vol. 86, no. 208, pp. 9–18, 2019, doi: 10.15446/DYNA.V86N208.72589.

[17] W. Earle, "Calhoun: The NPS Institutional Archive DSpace Repository Thermoelectric cooler design." [Online]. Available: http://hdl.handle.net/10945/23788

[18] P. I. Mani, "Design, Modeling and Simulation of a Thermoelectric Cooling Design, Modeling and Simulation of a Thermoelectric Cooling System (TEC) System (TEC)." [Online]. Available: https://scholarworks.wmich.edu/masters_theses

[19] "Thermoelectric Cooling Modules," *Mathematical Modeling of Thermoelectric Cooling Modules https://thermal.ferrotec.com/technology/thermoelectric-reference-guide/thermalref11/*, pp. 1–99, 2019.

[20] I. T. Nazzal, T. K. Salem, and R. R. J. al Doury, "Theoretical Investigation of a Pin Fin Heat Sink Performance for Electronic Cooling using Different Alloys Materials," *IOP Conference Series: Materials Science and Engineering*, vol. 1094, no. 1, p. 012087, Feb. 2021, doi: 10.1088/1757-899x/1094/1/012087.

[21] J. Chen and J. A. Schouten, "Comment on 'A new approach to optimum design in thermoelectric cooling systems' [J. Appl. Phys. 80, 5494 (1996)]," *Journal of Applied Physics*, vol. 82, no. 12. American Institute of Physics Inc., pp. 6368–6369, Dec. 15, 1997. doi: 10.1063/1.366517.

[22] A. Elghool, F. Basrawi, T. K. Ibrahim, K. Habib, H. Ibrahim, and D. M. N. D. Idris, "A review on heat sink for thermo-electric power generation: Classifications and parameters affecting performance," *Energy Conversion and Management*, vol. 134. Elsevier Ltd, pp. 260–277, 2017. doi: 10.1016/j.enconman.2016.12.046.

[23] "HEAT TRANSFER, TENTH EDITION by J.P.Holman," 2008.

[24] "Heat Transfer,sixth Edition, by J.P.Holman 1986".

[25] Y. A. Cengel, "YUNUS A. CENGEL Heat transfer Steady versus Transient Heat Transfer apractical approach."